

Experimental and theoretical studies on the elasticity of molybdenum to 12 GPa

Wei Liu,^{1,a)} Qiong Liu,¹ Matthew L. Whitaker,^{1,2} Yusheng Zhao,³ and Baosheng Li¹

¹Mineral Physics Institute, Stony Brook University, Stony Brook, New York 11794, USA

²Department of Geosciences, Stony Brook University, Stony Brook, New York 11794, USA

³LANSCE, Los Alamos National Lab, Los Alamos, New Mexico 87545, USA

(Received 26 May 2009; accepted 1 July 2009; published online 19 August 2009)

Experiments have been conducted to measure compressional (V_P) and shear wave (V_S) velocities as well as unit-cell volumes (densities) of molybdenum to 12.0 GPa at room temperature using ultrasonic interferometry in conjunction with synchrotron x-radiation. Both V_P and V_S as well as the adiabatic bulk (K_S) and shear (G) moduli exhibit monotonic increase with increasing pressure. A finite strain equation of state analysis of the directly measured velocities and densities yields $K_{S0} = 260.7(5)$ GPa, $G_0 = 125.1(2)$ GPa, $K'_{S0} = 4.7(1)$, and $G'_0 = 1.5(1)$ for the elastic bulk and shear moduli and their pressure derivatives at ambient conditions. Complimentary to the experimental data, V_P and V_S as well as the elastic bulk and shear moduli were also computed using density functional theory (DFT) at pressures comparable to the current experiment. Comparing with experimental results, the velocities and elastic moduli from DFT calculations exhibit close agreement with the current experimental data both in their values as well as in their pressure dependence. © 2009 American Institute of Physics. [DOI: 10.1063/1.3197135]

I. INTRODUCTION

Molybdenum is a body-centered-cubic (bcc) 4d transition metal with extensive application in modern technology for its extreme stability and refractory properties. The equation of state (EOS) of molybdenum (Mo) at high pressures was used to calibrate the ruby fluorescence pressure scale, which is widely used as pressure calibrant in diamond-anvil cell experiments.¹ Numerous investigations have been performed on molybdenum, including ultrasonic measurements of elastic constants at high temperature or at high pressure,^{2–6} static compression experiments,^{7–12} shock wave experiments,^{13–15} and theoretical calculations.^{16–18}

Elastic bulk (K_S) and shear (G) moduli and their pressure derivatives are important parameters in understanding the structural behavior and physical properties of materials under compression. The elastic properties of Mo have been measured only up to 0.5 GPa.⁶ Recently, the state-of-the-art techniques developed in our laboratory have enabled simultaneous measurements of elastic compressional (P) and shear (S) wave velocities, and hence the elastic properties of materials at high pressure and high temperature using combined ultrasonic interferometry, x-ray diffraction, and x-radiography in large-volume high-pressure apparatus.¹⁹

In this paper, we present the results of the compressional and shear wave velocities to 12 GPa from both experiments and density functional theory (DFT) calculations. The elastic bulk and shear moduli and their pressure derivatives are derived from the measured V_P - V_S volume data using third-order finite strain equations of state; the results are compared with those from DFT calculations as well as those from previous experimental studies.

II. EXPERIMENT AND COMPUTATION

The polycrystalline molybdenum rod (Alfa, 99.95%) with a diameter of 2.0 mm was used in this investigation. Using the Archimedes' method, a bulk density of 9.942(10) g cm⁻³ was obtained, which is 97.3% of the theoretical x-ray density of 10.219 g cm⁻³. To minimize the acoustic energy loss, all surfaces along the acoustic travel path, including the tungsten carbide (WC) anvil on which the transducer was mounted, and both sides of the buffer rod and sample, were polished using 1 μm diamond paste in final finish. The flatness and parallelism of those surfaces are within 0.5 and 2.5 μm.

Compressional (P) and shear (S) wave velocities at high pressure were measured using ultrasonic interferometry techniques in conjunction with *in situ* x-ray diffraction and radiography in a DIA-type, multianvil, high pressure apparatus (SAM85) installed on the superconducting wiggler beamline (X17B2) of the National Synchrotron Light Source at the Brookhaven National Laboratory. Details of this experimental setup and the ultrasonic interferometry have been described elsewhere.^{19–21} The sample length at high pressure was directly obtained by the x-radiographic imaging method, the precision of this direct measurement of sample length was reported to be 0.2%–0.4%.¹⁹

X-ray diffraction patterns for the sample were recorded in the energy dispersive mode using a solid state Ge detector. The incident x-ray beam was collimated to 0.2 mm by 0.1 mm and the diffraction angle was set at $2\theta = 6.52^\circ$. The (110), (211), (220), and (310) diffraction lines were used in the refinement of unit-cell volumes for Mo, with a relative standard deviation less than 0.1%.

Theoretical calculations were performed within the framework of DFT using all-electron full potential linear augmented plane wave plus local orbitals method as em-

^{a)}Electronic mail: weiliu3@notes.cc.sunysb.edu.

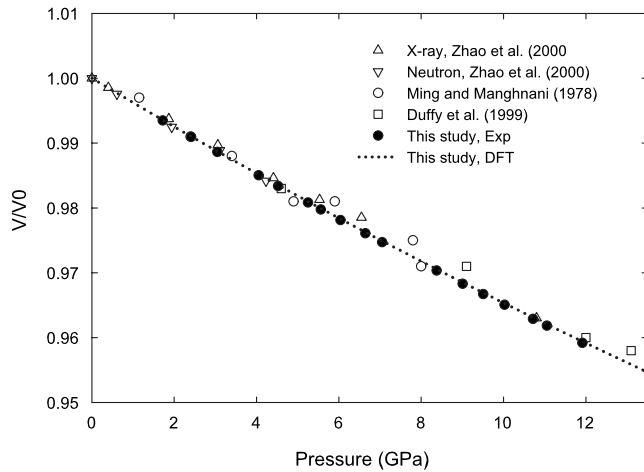


FIG. 1. Variation of unit-cell volumes of molybdenum as a function of pressure. Symbols are from experimental studies, dotted line represents the results from current DFT calculations.

ployed in WIEN2K code.^{22,23} The unit cell is divided into non-overlapping atomic spheres (muffin-tin, radius R_{MT}) and an interstitial region where Kohn–Sham wave functions,²⁴ charge density and potential are expanded in different sets of basis functions. The charge density and potential are expanded into lattice harmonics inside muffin-tin spheres and as a Fourier series in the remaining space. A maximum quantum number of ten was used for the atomic wave functions inside the muffin-tin sphere. The generalized gradient approximation of Perdew *et al.*²⁵ was used for the exchange-correlation functionals. A sphere radius of 2.4 a.u. was used in the current calculation, and the Brillouin zone was sampled by 10 000 k -points (268 in the irreducible wedges). The plane wave cutoff was set by $R_{\text{MT}}^* K_{\text{max}} = 8$ where K_{max} is the maximum k vector in the basis set. The largest vector in the charge density Fourier expansion was $G_{\text{max}} = 14$ bohr⁻¹. The criterion for self-consistency energy convergence was 1 μRy . Convergence tests were conducted by using different values of $R_{\text{MT}}^* K_{\text{max}}$ and k -points to make sure the self-consistent force calculations is well converged with those used in the current calculations. The elastic constants were calculated using the procedures described in Ref. 23, in which a series of energy minimizations were performed after applying small strains to the Mo unit cells and the elastic constants were then derived from the second derivatives of the energy with respect to the applied strains. The bulk and shear moduli corresponding to polycrystalline sample were obtained using a Voigt–Reuss–Hill average method. The same values of $R_{\text{MT}}^* K_{\text{max}}$ were used for the current calculations at all pressures.

III. RESULTS AND DISCUSSION

The x-ray powder diffraction patterns show that the Mo sample remains in the bcc phase up to the peak pressure of the current study (12.0 GPa). The refined unit-cell volumes show a smooth decrease with increasing pressure (Fig. 1). We obtain a value of 31.175(25) \AA^3 from our experiment for the unit-cell volume at ambient conditions, which is in good agreement with the value of 31.161 \AA^3 from Pearson²⁶

(1958) and Neutron diffraction result of 31.181(3) \AA^3 from Zhao *et al.*¹⁰ (2000), and within mutual uncertainties with the x-ray diffraction result of 31.150 \AA^3 (3) from Zhao *et al.* (2000).¹⁰ Our DFT calculation at 0 K yields a value of 31.63 \AA^3 which is in agreement with experimental data within 1.5%. The unit-cell volumes of Mo as a function of pressure are compared with previous studies in Fig. 1. The 300 K compression curve from the current experiment is in excellent agreement with previous results,^{7,9,10} although some previous data show minor scattering at the pressure range from 5 to 9 GPa. The current experimental data also show an excellent agreement with those from DFT calculations at ground state (Fig. 1).

Compressional and shear wave velocities as well as the adiabatic bulk ($K_S = L - 4G/3 = \rho V_P^2 - 4G/3$) and shear ($G = \rho V_S^2$) moduli at high pressures are obtained from the measured sample lengths, travel times, and densities (Table I). As shown in Fig. 2, both V_P and V_S exhibit linear increase with pressure at room temperature. The pressure dependence is in excellent agreement with those from DFT calculations, although the values of the velocities from DFT calculations (at 0 K) are slightly higher than the experimental data at temperature of 300 K (Fig. 2).

To obtain the zero-pressure adiabatic bulk and shear moduli as well as their respective pressure derivatives, the velocity and density data can be fitted simultaneously to the finite strain Eqs. (1) and (2) without the input of pressure,²⁷

$$\rho V_P^2 = (1 - 2\varepsilon)^{5/2}(L1 + L2\varepsilon), \quad (1)$$

$$\rho V_S^2 = (1 - 2\varepsilon)^{5/2}(M1 + M2\varepsilon), \quad (2)$$

in which $M1 = G_0$, $M2 = 5G_0 - 3K_{S0}G_0'/L1 = K_{S0} + 4G_0/3$, and $L2 = 5L1 - 3K_{S0}(K_{S0}' + 4G_0'/3)$. The strain ε is defined as $[1 - (V_0/V)^{2/3}]/2$. The fitted coefficients, $L1$, $L2$, $M1$, and $M2$, are used for the calculation of the zero-pressure adiabatic bulk and shear moduli (K_{S0} and G_0), as well as their pressure derivatives (K_{S0}' and G_0').

The velocity and density data from our experiments are fitted to Eqs. (1) and (2) by minimizing the difference between the calculated and the observed compressional and shear wave velocities, yielding $K_{S0} = 260.7(5)$ GPa, $G_0 = 125.1(2)$ GPa, $K_{S0}' = 4.7(1)$, and $G_0' = 1.5(1)$. These parameters reproduce the observed compressional and shear wave velocities remarkably well in the entire pressure range, with a RMS (root mean squares) misfit of 0.006 km s⁻¹ for V_P and 0.002 km s⁻¹ for V_S , respectively. These results, together with those from the current DFT calculations, are compared with previous results in Table II.

The ambient pressure adiabatic bulk modulus K_{S0} , 260.7 GPa, agrees very well with previous values (259.3–263.8 GPa) from acoustic measurements on single crystal,^{3–6} within their respective estimates of error ($\sim 1\%$ – 2%). One exception is that the K_{S0} value of Bolef and de Klerk² (1962), which is only in marginal agreement with the upper bound of the current data as well as other single crystal acoustic measurements. The zero-pressure adiabatic shear modulus G_0 from our measurement is in excellent agreement with the Voigt–Reuss–Hill (VRH) averages of shear moduli from pre-

TABLE I. Experimental ultrasonic data and unit-cell parameters of molybdenum.

P^a (GPa)	L (mm)	$2tp$ (μ s)	$2ts$ (μ s)	V_p (km s $^{-1}$)	V_s (km s $^{-1}$)	V (\AA^3)	ρ (g cm $^{-3}$)	K_S (GPa)	G (GPa)
1.7	0.7631	0.2333	0.4326	6.542	3.528	30.972	10.286	269.5	128.0
2.4	0.7616	0.2323	0.431	6.557	3.534	30.893	10.312	271.4	128.8
3.1	0.7602	0.2309	0.4293	6.585	3.542	30.820	10.337	275.3	129.7
4.1	0.7597	0.2299	0.4276	6.609	3.553	30.708	10.374	278.5	131.0
4.6	0.7587	0.2287	0.426	6.635	3.562	30.656	10.392	281.7	131.9
5.3	0.7587	0.2279	0.425	6.658	3.570	30.577	10.419	284.8	132.8
5.6	0.7582	0.2271	0.4239	6.677	3.577	30.544	10.43	287.1	133.5
6.1	0.7577	0.2263	0.4228	6.696	3.584	30.493	10.448	289.5	134.2
6.7	0.7577	0.2257	0.422	6.714	3.591	30.429	10.47	292.0	135.0
7.1	0.7582	0.2253	0.4212	6.726	3.598	30.387	10.484	293.3	135.7
8.4	0.7592	0.2245	0.4202	6.763	3.614	30.251	10.531	298.3	137.6
9.1	0.7592	0.2239	0.4192	6.782	3.622	30.187	10.553	300.8	138.4
9.6	0.7592	0.2231	0.4182	6.806	3.631	30.137	10.571	303.8	139.4
10.1	0.7587	0.2223	0.4174	6.826	3.635	30.086	10.589	306.8	139.9
10.8	0.7582	0.2215	0.4162	6.846	3.643	30.018	10.613	309.6	140.9
11.1	0.7587	0.2209	0.4156	6.869	3.651	29.985	10.625	312.5	141.6
12.0	0.7582	0.2199	0.4144	6.896	3.659	29.903	10.654	316.5	142.6

^a $P = -3K_{S0}\epsilon(1-2\epsilon)^{5/2}[1+3(4-K'_{S0})\epsilon/2]$ (Ref. 27). Values in parentheses are 1σ error in the last digits. The uncertainty of the unit-cell volumes are less than 0.15%. Travel times have 1σ of ~ 0.4 ns for S wave, and ~ 0.2 ns for P wave. The uncertainties are less than 0.5% in velocities and less than 1.5% in the derived elastic moduli. The densities at pressures are calculated using the unit-cell volumes and the theoretical density at room temperature ($\rho = \rho_0^*V/V_0$).

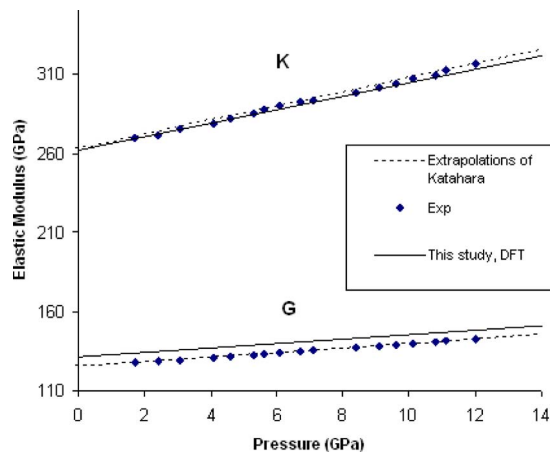


FIG. 2. (Color online) Elastic compressional (V_p) and shear (V_s) wave velocities for molybdenum as a function of pressure from the current ultrasonic and x-ray measurements to 12.0 GPa (symbols) and from DFT calculations (lines).

TABLE II. Elastic moduli and their pressure derivatives of Mo.

References	K_{S0}	G_V	G_R	G_{VRH}	K'_{S0}	G'	K_T	K'_T	Notes
2	268.3	124.5	121.0	122.7					Single crystal, ultrasonic, 77–500 K
3	261.9	126.7	126.4	126.6					Single crystal, ultrasonic, 4.2–300 K
4	259.3	126.2	122.9	124.5					Single crystal, pulse echo, –198–650 C
4	261.6	125.8	122.6	124.2					Single crystal, thin rod resonance, –198–650 C
5	263.8	126.4	123.2	124.8					Single crystal, ultrasonic, –190–100 C
6	262.6	126.0	122.7	124.4	4.44	1.43			single crystal, ultrasonic, to 0.5 GPa
7	267(11)				[4.46]				DAC, to 10 GPa
13							267	3.9	Shock wave experiment
8							262.8	3.95	DAC, to 272 GPa
10							268 (1)	3.81 (6)	EoS, x-ray, to 10 GPa and 1475 K, combine shock data
10							264 (1)	4.05 (2)	EoS, x-ray, to 10 GPa and 1475 K, combine shock data
10							266(9)	4.1(9)	EoS, x-ray, to 10 GPa and 1475 K
This study	260.7(5)			125.1(2)	4.7(1)	1.5(1)			Ultrasonic, 3rd FS, to 12 GPa
This study	261.0(5)			125.3(2)	4.54(1)	1.45(1)			Ultrasonic, linear fit to 12 GPa
This study							261.9	4.5	DFT

vious single crystal elastic constant measurements,^{3–6} except that of Bolef and de Klerk² (1962), with which the agreement is within $\sim 2\%$.

Our experimental results for the pressure derivatives of the bulk and shear moduli, $K'_{S0}=4.7(1)$ and $G'_0=1.5(1)$, appear to be slightly higher than the respective value of 4.44 and 1.43 derived using experimental data up to 0.5 GPa from Katahara *et al.* (1979). It should be noted that the current results are derived from a finite strain fit instead of a linear fit to pressure. If we fit the current elastic moduli data with a linear expression of pressure as in Katahara *et al.* (1979), we obtain $K_{S0}=261.0$ GPa, $G_0=125.3(2)$ GPa, $K'_{S0}=4.54(1)$, and $G'_0=1.45(1)$ (see Table II), which is in excellent agreement with those from Katahara *et al.* (1979). The close agreement of K_{S0} , G_0 , K'_{S0} , and G'_0 derived from the current measurements with the results of Katahara *et al.* (1979) sug-

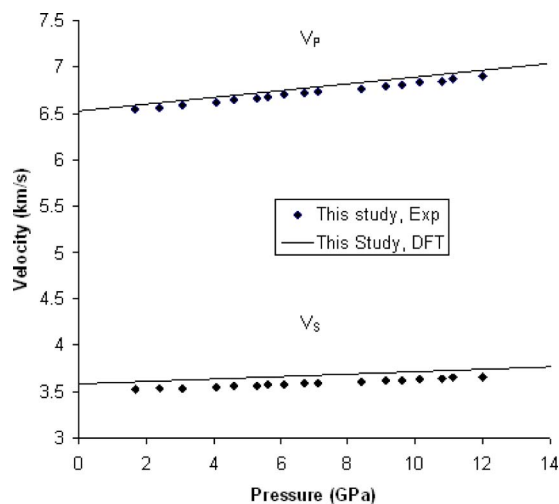


FIG. 3. (Color online) Variation of bulk (K_S) and shear (G) modulus for molybdenum as a function of pressure. Symbols are from experimental studies, solid line represents the results from current DFT calculations, and dashed lines are the extrapolations of results from Katahara *et al.* (1979).

gests that bulk and shear moduli of the current measurements are in excellent agreement with those extrapolated values using the results of Katahara *et al.* (1979) and the effect of the second pressure derivatives (K'' and G'') in the current pressure range (12.0 GPa) is negligible (Fig. 3).

As seen in Fig. 3, the current experimental observation of the pressure dependence for the bulk and shear moduli is also supported by our DFT calculations. Quantitatively, with the density and elastic moduli data from DFT calculations, we can perform finite strain fit to determine the bulk and shear moduli and their pressure derivatives following the procedures described above for the analysis of experimental data. The fitting results $K_{S0}=259(5)$ GPa, $G_0=130(2)$ GPa, $K'_{S0}=4.4(7)$, and $G'_0=1.7(3)$, compare very well with the experimental data on the pressure derivative of the bulk and shear moduli. By comparison, the x-ray diffraction studies (Refs. 8, 10, and 13) appear to have a lower K'_0 of 3.8–4.1 (we ignored the small difference between K'_{S0} and K'_{T0}) but with a slightly higher K_0 (263–268 GPa), this could be due to the tradeoff between K_0 and K'_0 in EOS analysis. If the value of $K'_0 \sim 3.9$ with $K_0=262.5$ GPa obtained from diamond anvil cell (DAC) measurements up to 272 GPa is as accurate as that from the current acoustic study, the apparent discrepancy in K'_0 may be attributed to the increased effect of the second order pressure derivatives (K'' and G'') at these extreme pressures.

ACKNOWLEDGMENTS

This research is supported by DoE/NNSA (Contract No. DEFG5206NA2621 to B.L.). We thank Michael Vaughan and Liping Wang for technical support at the X17B2 beamline. These experiments were carried out at the National Synchrotron Light Source (NSLS), which is supported by the U.S. Department of Energy, Division of Materials Sciences and Division of Chemical Sciences under Contract No. DE-AC02-76CH00016. X-17B2 is supported by COMPRES. Mineral Physics Institute Publication No. 478.

- ¹H. K. Mao, P. M. Bell, J. W. Shaner, and D. J. Steinberg, *J. Appl. Phys.* **49**, 3276 (1978).
- ²D. I. Bolef and J. de Klerk, *J. Appl. Phys.* **33**, 2311 (1962).
- ³F. H. Featherston and J. R. Neighbours, *Phys. Rev.* **130**, 1324 (1963).
- ⁴J. M. Dickinson and P. E. Armstrong, *J. Appl. Phys.* **38**, 602 (1967).
- ⁵D. L. Davidson and F. R. Brotzen, *J. Appl. Phys.* **39**, 5768 (1968).
- ⁶K. W. Katahara, M. H. Manghnani, and E. S. Fisher, *J. Phys. F: Met. Phys.* **9**, 773 (1979).
- ⁷L. C. Ming and M. H. Manghnani, *J. Appl. Phys.* **49**, 208 (1978).
- ⁸Y. K. Vohra and A. L. Ruoff, *Phys. Rev. B* **42**, 8651 (1990).
- ⁹T. S. Duffy, G. Shen, J. Shu, H. K. Mao, R. J. Hemley, and A. K. Singh, *J. Appl. Phys.* **86**, 6729 (1999).
- ¹⁰Y. Zhao, A. C. Lawson, J. Zhang, B. I. Bennett, and R. B. Von Dreele, *Phys. Rev. B* **62**, 8766 (2000).
- ¹¹D. L. Farber, M. Krisch, D. Antonangeli, A. Beraud, J. Badro, F. Occelli, and D. Orlikowski, *Phys. Rev. Lett.* **96**, 115502 (2006).
- ¹²R. Selva Vennila, S. R. Kulkarni, S. K. Saxena, H.-P. Liermann, and S. V. Sinogeikin, *Appl. Phys. Lett.* **89**, 261901 (2006).
- ¹³W. J. Carter, S. P. Marsh, J. N. Fritz, and R. G. McQueen, *NBS Spec. Publ.* **36**, 147 (1971).
- ¹⁴G. H. Miller, T. J. Ahrens, and E. M. Stöpler, *J. Appl. Phys.* **63**, 4469 (1988).
- ¹⁵R. S. Hixson, D. A. Boness, and J. W. Shaner, *Phys. Rev. Lett.* **62**, 637 (1989).
- ¹⁶B. K. Godwal and R. Jeanloz, *Phys. Rev. B* **41**, 7440 (1990).
- ¹⁷J. A. Moriarty, *Phys. Rev. B* **45**, 2004 (1992).
- ¹⁸B. Belonoshko, S. I. Simak, A. E. Kochetov, B. Johansson, L. Burakovsky, and D. L. Preston, *Phys. Rev. Lett.* **92**, 195701 (2004).
- ¹⁹B.-S. Li, J. Kung, and R. C. Liebermann, *Phys. Earth Planet. Inter.* **143–144**, 559 (2004).
- ²⁰R. C. Liebermann and B. Li, in *Ultra-high Pressure Mineralogy: Physics and Chemistry of the Earth's Deep Interior*, Reviews in Mineralogy Vol. 37 edited by R. J. Hemley (Mineralogical Society of America, Washington, D. C., 1998).
- ²¹W. Liu and B. Li, *Appl. Phys. Lett.* **93**, 191904 (2008).
- ²²K. Schwarz, *J. Solid State Chem.* **176**, 319 (2003).
- ²³P. Blaha, K. Schwarz, P. Sorantin, and S. B. Trickey, *Comput. Phys. Commun.* **59**, 399 (1990).
- ²⁴W. Kohn and L. J. Sham, *Phys. Rev.* **140**, A1133 (1965).
- ²⁵J. P. Perdew, K. Burke, and M. Ernzerhof, *Phys. Rev. Lett.* **77**, 3865 (1996).
- ²⁶W. B. Pearson, *Handbook of Lattice Spacings and Structures of Metals and Alloys* (Pergamon, New York, 1958), Vol. 1.
- ²⁷G. F. Davies and A. M. Dziewonski, *Phys. Earth Planet. Inter.* **10**, 336 (1975).